ABS and Active Suspension Control via High Order Sliding Modes and Linear Geometric Methods for Disturbance Rejection

Juan Diego Sánchez-Torres[1], Alexander G. Loukianov[2], Marcos I. Galicia[3], Javier Ruiz [4] and Jorge Rivera[5]
[1−4] Department of Electrical Engineering, CINVESTAV Unidad Guadalajara, 45015 México
e-mail: [dsanchez[1], louk[2], mgalicia[3], ruiz[4]]@gdl.cinvestav.mx
[5] Centro Universitario de Ciencias Exactas e Ingenierías de la Universidad de Guadalajara, 44430 México
e-mail: jorge.rivera@cucei.udg.mx

***Abstract*— In this work, high order sliding mode techniques are used to control an Anti-lock Brake System (ABS) which is assisted with an active suspension. The main objective is to modify the slip rate of a vehicle and ensure a shorter stopping distance in the braking process. The control system is designed in independent way for the ABS and the suspension subsystem. For the ABS subsystem a second order sliding mode controller is used. On the other hand, for the active suspension subsystem the supertwisting algorithm combined with regular form and linear geometric techniques is proposed. The use of sliding mode controllers allows that both closed-loop subsystems are robust against a class of external perturbations and system uncertainties, furthermore the chattering effect is reduced and higher tracking accuracy is obtained. The effectiveness of the proposed control strategy is confirmed via simulations.**

Keywords: Brake Control, Antilock Braking Systems (ABS), Sliding Mode Control, Automotive Control.

I. INTRODUCTION

Technology advances quickly every day, researchers of diverse areas are looking for alternatives to accomplish common tasks using a big variety of methods. Since the vehicles were made, they have been changed constantly. Now, they have more quality, they are safer, provide more comfort, have a better performance and they are more effective. The breaking process is one of the most important topics to consider in safety, there are several kinds of breaking systems e.g. the ABS, and traction control system. One of the objectives of the active suspension is to guarantee the improvement of the ride quality namely the comfort for the passengers. The ABS as a control problem consists in imposing a desired vehicle motion to enhance the vehicle stability. There are different mathematical models of the ABS system, however, all they content high non-linearities and uncertainties which are the main difficulties arising in the ABS design and control. For the whole system control design is necessary to cope with the disturbance due to road friction which is unknown. Therefore, the researchers in area of robust control consider the ABS and active suspension as interesting problems to be solved.

Sliding mode (SM) control [1] provides robustness properties against uncertainties in system parameters and external disturbances, however, SM has a drawback: high frequency switching may become destructive for actuators of the plant or may cause system resonance via excitation of neglected or unmodeled dynamics of the system under control. These dangerous vibrations are called the chattering effect. High Order SM (HOSM) [2] improve accuracy of standard SM, HOSM has the main sliding-mode features namely that preserves robustness properties, finite time convergence, furthermore chattering effect is reduced considerably. Several works have been reported in the literature using the sliding mode technique to a slip-ratio control of ABS, for example [3], [4], [5], [6]. For the active suspension case a similar approach is used in the [7]. In [8] a backstepping design is applied to ABS and active suspension as a whole system, in this case the road disturbances have been assumed known in order to propose the control law. However, in most cases these two systems are treated independently.

In this paper, we use HOSM techniques to design a controller to achieve the relative slip tracks a desired trajectory to obtain a shorter stopping distance. In the other hand, a combination of HOSM namely supertwisting, regular form [9] and geometric linear [10] approaches is used to design the active suspension controller, which guarantees the passenger comfort and helps to improve the braking process. As a result the vehicle dynamic, i.e., the vehicle velocity and horizontal position, on the designed SM manifolds becomes asymptotically stable with disturbance attenuation, ensuring an stable tracking error.

The paper is organized as follows. The mathematical

model for the longitudinal movement of a vehicle, including the brake and active suspension systems is presented in Section II. In Section III the HOSM controllers with special emphasis in the design of sliding surface for active suspension are shown. The simulation results are presented in Section IV to show the robustness and performance of the proposed control strategy. Finally, some conclusions are presented in Section V.

II. MATHEMATICAL MODEL

This section presents a dynamic model of a vehicle active suspension and ABS subsystems similar as is used in [8]. In this work, we consider a quarter of vehicle model, this model includes the active suspension, the pneumatic brake system, the wheel motion and the vehicle motion. Now we study the task of controlling the wheels rotation, such that, the longitudinal force due to the contact of the wheel with the road is near from the maximum value in a period of time valid for the model. This effect is reached as a result of the ABS valve effort.

A. Active suspension model

The quarter-car active suspension is a 2-DOF mechanical system shown in Fig. 1.

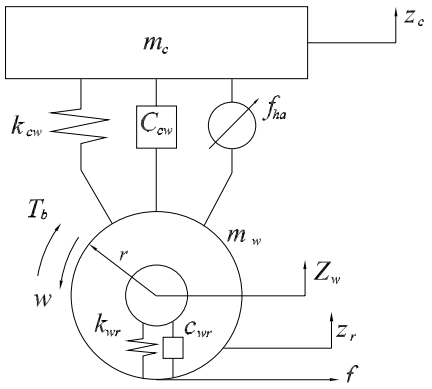

Fig. 1: Active suspension scheme

this system connects the car body and the wheel masses and is modeled as a linear viscous damper and a spring elements, whereas the tire is represented as a linear spring and damping elements. The motion equations for this system are represented by

$$\begin{aligned} m_c\ddot{z}_c &= -K_{cw}(z_c - z_w) - C_{cw}(\dot{z}_c - \dot{z}_w) + f_{ha} \\ m_w\ddot{z}_w &= K_{cw}(z_c - z_w) + C_{cw}(\dot{z}_c - \dot{z}_w) \\ &\quad -K_{wr}(z_w - z_r) - C_{wr}(\dot{z}_w - \dot{z}_r) - f_{ha} \end{aligned} \tag{1}$$

where m_c and m_w the mass of the car an the wheel, respectively, z_c is the car vertical displacement, z_w is the wheel vertical displacement, K_{cw} and K_{wr} are the spring coefficients, C_{cw} and C_{wr} are the damping coefficients, z_r is the disturbance due to road and f_{ha} is the force of the hydraulic actuator.

B. Pneumatic brake system equations

The specific configuration of this system considers the brake disk, which holds the wheel, as a result of the increment of the air pressure in the brake cylinder. The entrance of the air trough the pipes from the central reservoir and the expulsion from the brake cylinder to the atmosphere is regulated by a common valve.

The time response of the valve is considered small, compared with the time constant of the pneumatic system.

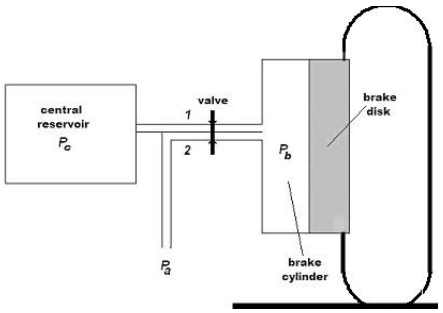

Fig. 2: Pneumatic brake scheme

Considering Fig. 2, we suppose the brake torque T_b is proportional to the pressure P_b in the brake cylinder

$$T_b = k_b P_b \tag{2}$$

with $k_b > 0$. For the brake system we use an approximated model of pressure changes in the brake cylinder due to the opening of the valve with a first order relation [11], this relation can be represented as

$$\tau\dot{P}_b + P_b = P_c \tag{3}$$

where τ is the time constant of the pipelines, P_c is the pressure inside the central reservoir. The atmospheric pressure, P_a, is considered equal to zero.

C. Wheel motion equations

To describe the wheel motion we use a partial mathematical model of the dynamic system as it is done in [12], [13], [14]. Considering the Fig. 2, the dynamics of the angular momentum variation relative to the rotation axis, are given by

$$J\dot{\omega} = rf(s) - b_b\omega - T_b \tag{4}$$

where ω is the wheel angular velocity, J is the wheel inertia moment, r is the wheel radius, b_b is a viscous friction coefficient due to wheel bearings and f is the contact force of the wheel.

The expression for longitudinal component of the contact force in the motion plane is

$$f(s) = \nu N_m \phi(s) \tag{5}$$

where ν is the nominal friction coefficient between the wheel and the road, N_m is the normal reaction force in the wheel and it is defined by $N_m = mg - K_{wr}(z_w - z_r) - C_{wr}(\dot{z}_w - \dot{z}_r)$, with g the gravity acceleration and m the mass supported on the wheel and it is given by $m = m_w + m_c/4$. The function $\phi(s)$ represents a friction/slip characteristic relation between the tire and road surface. Here, we use the *Pacejka formula* [15], defined as follows

$$\phi(s) = D\sin(C\text{atan}(Bs - E(Bs - \text{atan}(Bs))))$$

.

In general, this model produces a good approximation of the tire/road friction interface. With the following parameters $B = 10$, $C = 1.9$, $D = 1$ and $E = 0.97$ that function represents the friction relation under a dry surface condition.

The slip rate s is defined as

$$s = \frac{v - r\omega}{v} \tag{6}$$

where v is the longitudinal velocity of the wheel mass center. The equations (4)-(6) characterize the wheel motion.

D. The vehicle motion equation

The vehicle longitudinal dynamics considered without lateral motion, are described by

$$M\dot{v} = -F(s) - F_a \tag{7}$$

where $M = 4m_w + m_c$ is the total vehicle mass; F_a is the aerodynamic drag force, which is proportional to the vehicle velocity and is defined as $F_a = \frac{1}{2}\rho C_d A_f (v + v_w)^2$, where ρ is the air density, C_d is the aerodynamic coefficient, A_f is the frontal area of vehicle, v_w is the wind velocity; and the contact force of the vehicle F is modeled of the form

$$F(s) = \nu N_M \phi(s) \tag{8}$$

where N_M is the normal reaction force of the vehicle, $N_M = Mg - K_{wr}(z_w - z_r) - C_{wr}(\dot{z}_w - \dot{z}_r)$.

E. State space equations

The dynamic equations of the whole system (3)-(7) can be rewritten using the state variables $\mathbf{x} = [x_1, x_2, x_3, x_4, x_5, x_6, x_7]^T = [z_c, \dot{z}_c, z_w, \dot{z}_w, \omega, P_b, v]^T$ results in the following form:

$$\begin{aligned}
\dot{x}_1 &= x_2 \\
\dot{x}_2 &= -a_1(x_1 - x_3) - a_2(x_2 - x_4) + b_1 u_s \\
\dot{x}_3 &= x_4 \\
\dot{x}_4 &= a_3(x_1 - x_3) + a_4(x_2 - x_4) \\
&\quad -a_5(x_3 - z_r) - a_6(x_4 - \dot{z}_r) - b_2 u_s \\
\dot{x}_5 &= -a_7 x_5 + a_8 f(s) - a_9 x_6 \\
\dot{x}_6 &= -a_{10} x_6 + b_3 u_b \\
\dot{x}_7 &= -a_{11} F(s) - f_w(x_7)
\end{aligned} \tag{9, 10}$$

with the outputs $y_1 = x_1$ and $y_2 = x_5$, where $a_1 = K_{cw}/m_c$, $a_2 = C_{cw}/m_c$, $a_3 = K_{cw}/m_w$, $a_4 = C_{cw}/m_w$, $a_5 = K_{wr}/m_w$, $a_6 = C_{wr}/m_w$, $a_7 = b_b/J$, $a_8 = r/J$, $a_9 = k_b/J$, $a_{10} = 1/\tau$, $a_{11} = 1/M$, $b_1 = 1/m_c$, $b_2 = 1/m_w$, $b_3 = 1/\tau$, $u_s = f_{ha}$, $u_b = P_c$ and $f_w(x_7) = \frac{1}{2M}(\rho C_d A_f)(x_7 + v_w)^2$.

III. CONTROL DESIGN

In this section, we use the concepts of regular form, SM and geometric linear control methods for the sliding surface for an active suspension controller design; and, then HOSM is applied to design an ABS controller. In this case, the form of the whole system (9)-(10) allows us to design both controllers in independent way.

A. Suspension Control

Define $\mathbf{x}_s = [x_1, x_2, x_3, x_4]$ and $\mathbf{p} = \begin{bmatrix} z_r & \dot{z}_r \end{bmatrix}^T$, then the subsystem (9) is represented as

$$\dot{\mathbf{x}}_s = \mathbf{A}_s \mathbf{x}_s + \mathbf{b}_s u_s + \mathbf{D}\mathbf{p} \tag{11}$$

where

$$\begin{aligned}
\mathbf{A}_s &= \begin{bmatrix} 0 & 1 & 0 & 0 \\ -a_1 & -a_2 & a_1 & a_2 \\ 0 & 0 & 0 & 1 \\ a_3 & a_4 & -a_3 - a_5 & -a_4 - a_6 \end{bmatrix} \\
\mathbf{b}_s &= \begin{bmatrix} 0 \\ b_1 \\ 0 \\ -b_2 \end{bmatrix}; \quad \mathbf{D} = \begin{bmatrix} 0 & 0 \\ 0 & 0 \\ 0 & 0 \\ a_5 & a_6 \end{bmatrix}.
\end{aligned}$$

with the output $y_1 = x_1$. Now, we define new variables $x_{r1} = x_1$, $x_{r2} = x_2 + \frac{b_1}{b_2} x_4$, $x_{r3} = x_3$ and $x_{r4} = x_4$; using the nonlinear transformation the system (11) is shown into regular form [9]

$$\dot{\mathbf{x}}_{r1} = \mathbf{A}_{11}\mathbf{x}_{r1} + \mathbf{A}_{12}\mathbf{x}_{r2} + \mathbf{D}_1\mathbf{p} \tag{12}$$

$$\dot{\mathbf{x}}_{r2} = \mathbf{A}_{21}\mathbf{x}_{r1} + \mathbf{A}_{22}\mathbf{x}_{r2} + \mathbf{D}_2\mathbf{p} + \mathbf{b}_2 u_s \tag{13}$$

which consists of the two blocks: (12) with $\mathbf{x}_{r1} = \begin{bmatrix} x_{r1} & x_{r2} & x_{r3} \end{bmatrix}^T$ and (13) with $\mathbf{x}_{r2} = [x_4]$, where

$$\mathbf{A}_{11} = \begin{bmatrix} 0 & 1 & 0 \\ a_3\frac{b_1}{b_2} - a_1 & a_4\frac{b_1}{b_2} - a_2 & a_1 - \frac{b_1}{b_2}(a_3 + a_5) \\ 0 & 0 & 0 \end{bmatrix},$$

$$\mathbf{A}_{12} = \begin{bmatrix} -\frac{b_1}{b_2} \\ a_2 - \frac{b_1}{b_2}(a_4 + a_6 - a_2) - a_4\left(\frac{b_1}{b_2}\right)^2 \\ 1 \end{bmatrix}, \quad \mathbf{A}_{21} = \begin{bmatrix} a_3 & a_4 & -a_3 - a_5 \end{bmatrix}, \quad \mathbf{A}_{22} = \begin{bmatrix} -a_4\left(\frac{b_1}{b_2} + 1\right) - a_6 \end{bmatrix},$$

$\mathbf{b}_2 = [-b_2]$, $\mathbf{D}_1 = \begin{bmatrix} 0 & 0 \\ \frac{b_1}{b_2}a_5 & \frac{b_1}{b_2}a_6 \\ 0 & 0 \end{bmatrix}$ and $\mathbf{D}_2 = \begin{bmatrix} a_5 & a_6 \end{bmatrix}$.

Then for the first block (12), the output can be regarded as $y_1 = \mathbf{c}\mathbf{x}_{r1}$, with $\mathbf{c} = \begin{bmatrix} 1 & 0 & 0 \end{bmatrix}$. The vector $\mathbf{x}_{r2}$ is handled as a virtual control in the first block and it is designed as a linear function of $\mathbf{x}_{r1}$

$$\mathbf{x}_{r2} = -\mathbf{C}_1\mathbf{x}_{r1} + \xi \tag{14}$$

where $\mathbf{C}_1$ are the feedback gains. In this work, we assume the matrix $(\mathbf{A}_{11} - \mathbf{A}_{12}\mathbf{C}_1)$ is Hurwitz, and the term ξ is chosen as $\xi = H_k^{-1} y_{1d}$ with $H_k = \mathbf{c}\left(\mathbf{A}_{12}\mathbf{C}_1 - \mathbf{A}_{11}\right)^{-1}\mathbf{A}_{12}$, yielding a constant stable response y_{1d}. Using (14), a sliding variable ψ is formulated as

$$\psi = \mathbf{x}_{r2} + \mathbf{C}_1\mathbf{x}_{r1} - \xi \tag{15}$$

and the dynamics of (15) are governed by

$$\begin{aligned} \dot{\psi} &= \left(\mathbf{C}_1\mathbf{A}_{11} + \mathbf{A}_{21}\right)\mathbf{x}_{r1} + \left(\mathbf{C}_1\mathbf{A}_{12} + \mathbf{A}_{22}\right)\mathbf{x}_{r2} \\ &\quad + \left(\mathbf{C}_1\mathbf{D}_1 + \mathbf{D}_2\right)\mathbf{p} + \mathbf{b}_2 u_s. \end{aligned} \tag{16}$$

To induce chattering reduced sliding mode on $\psi = 0$, the super-twisting control algorithm [16, Chap. 2] is applied

$$\begin{aligned} u_s &= -\mathbf{b}_2^{-1}\Big[-\lambda_{s1}\left|\psi\right|^{\frac{1}{2}}\operatorname{sign}(\psi) + u_{s2} \\ &\quad - \left(\mathbf{C}_1\mathbf{A}_{11} + \mathbf{A}_{21}\right)\mathbf{x}_{r1} - \left(\mathbf{C}_1\mathbf{A}_{12} + \mathbf{A}_{22}\right)\mathbf{x}_{r2}\Big] \end{aligned} \tag{17}$$

$$\dot{u}_{s2} = -\lambda_{s2}\operatorname{sign}(\psi) \tag{18}$$

where $\lambda_{s1} > 0$, $\lambda_{s2} > 0$ are control gains. The stability condition for the closed-loop system (16) and (17) can be obtained via the transformation $q_s = \left(\mathbf{C}_1\mathbf{D}_1 + \mathbf{D}_2\right)\mathbf{p} - \lambda_{s2}\int_0^t \operatorname{sign}(\psi)\,dt$ to

$$\begin{aligned} \dot{\psi} &= -\lambda_{s1}\left|\psi\right|^{\frac{1}{2}}\operatorname{sign}(\psi) - q_s \\ \dot{q}_s &= -\lambda_{s2}\operatorname{sign}(\psi) + \left(\mathbf{C}_1\mathbf{D}_1 + \mathbf{D}_2\right)\dot{\mathbf{p}}. \end{aligned} \tag{19}$$

We assume that $\left|\left(\mathbf{C}_1\mathbf{D}_1 + \mathbf{D}_2\right)\dot{\mathbf{p}}\right| < L < \infty$ and choosing $\lambda_{s2} > 5L$ and, $32L \leq \lambda_{s1}^2 \leq 8\left(\lambda_{s2} - L\right)$ then, the system (19) is finite time globally stable [17], i.e, its solution converges in finite time to the origin $(\psi, q_s) = (0, 0)$. The sliding motion on $\psi = 0$ is given by (12) and (14), in this way the SM equation is

$$\dot{\mathbf{x}}_{r1} = \left(\mathbf{A}_{11} - \mathbf{A}_{12}\mathbf{C}_1\right)\mathbf{x}_{r1} + \mathbf{A}_{12}\xi + \mathbf{D}_1\mathbf{p}. \tag{20}$$

At this point, to reject the unmatched unknown perturbation $\mathbf{p}$ in the SM equation (20), we applied the well known geometrical approach [10]. The disturbance $\mathbf{p}$ can be rejected preserving SM equation stability if and only if the image of the matrix associated to the disturbance, $\operatorname{Im}\mathbf{D}_1$, belongs to $\mathbf{V}_g^*$, the so-called maximal $(\mathbf{A}_{11}, \mathbf{A}_{12})$-invariant subspace contained in the kernel of the output $y_1 = x_{r1} = \begin{bmatrix} 1 & 0 & 0 \end{bmatrix}\mathbf{x}_{r1}$.

It can be seen that this problem is solvable, since clearly $\operatorname{Im}\mathbf{D}_1 = \operatorname{span}\left\{\tilde{\mathbf{D}}_1\right\}$ belongs to $\mathbf{V}_g^* = \operatorname{span}\left\{\mathbf{V}_g^{*(1)}, \mathbf{V}_g^{*(2)}\right\}$ with $\tilde{\mathbf{D}}_1 = \begin{bmatrix} 0 & 1 & 0 \end{bmatrix}^T$, $\mathbf{V}_g^{*(1)} = \begin{bmatrix} 0 & 1 & 0 \end{bmatrix}^T$ and $\mathbf{V}_g^{*(2)} = \begin{bmatrix} 0 & 0 & 1 \end{bmatrix}^T$.

Then, using the virtual control $\mathbf{x}_{r2}$ (14), which produces $\mathbf{V}_g^*$ to be SM equation (20) invariant, the output $y_1 = x_{r1}$ is not affected at all by the signal $\mathbf{p}$, i.e, this control rejects the disturbance $\mathbf{p}$ in the SM equation. Notice that this control renders the system (20) maximally non-observable by canceling out the zeros associated to the transfer function between $\mathbf{p}$ and $y_1 = x_{r1}$ with closed-loop poles. The closed-loop system (20) is stable, because these zeros are stable, and the remaining pole is located in a suitable stable position.

B. ABS Control

In this section we present a second order sliding mode control design for the brake system based on the dynamics (10), we suppose that x_5, x_7, s are known. Taking in account the direct action of the pressure P_b on the brake cylinder over the wheels motion, we define the output tracking error as

$$\sigma \triangleq x_5 - \frac{1 - s^*}{r}x_7, \tag{21}$$

which has relative degree two. We will use the following assumptions:

- **A1** For some $K_m, K_M, C_m \geq 0$, we have that:

$$0 < K_m \leq \frac{\partial\sigma^{(2)}}{\partial u} \leq K_M, \quad \left|\sigma^2|_{u=0}\right| \leq C_m \tag{22}$$

- **A2** The trajectories of subsystem (10 are infinitely extensible in time for any Lebesgue-measurable bounded control.

Considering (9), and (10), we take the derivative of the tracking error (21)

$$\begin{aligned} \dot{\sigma} &= -a_7x_5 + a_8 f(s) - a_9x_6 - \frac{1 - s^*}{r}\dot{x_7} + \frac{x_7}{r}\dot{s}^* \\ &= -a_7x_5 + a_8 v N_m \phi(x_5, x_7) \\ &- c_4 a_{11} v N_M \phi(x_5, x_7) + c_4 f_w(x_7) - a_9x_6 \\ &= f_1(x_5, x_7) + b_4x_6 + \Delta_1 \end{aligned} \tag{23}$$

where $f_1(x_5, x_7) = c_4\left[a_{11}\nu N_M\phi(s) - f_w(x_7)\right] - a_7x_5 + a_8\nu N_m\phi(s)$, $b_4 = -a_9$, and $c_4 = \frac{1-s^*}{r}$. We consider that the term Δ_1 contains the reference derivative $\dot{s}^*$, the inevitable changes of the friction parameter ν, the wind speed v_w, the influence of z_r, $\dot{z}_r$ on the high nonlinear $F(s)$. Hence, Δ_1 will be considered as an unmatched and bounded perturbation term.

Now if we take the second derivative of σ

$$\ddot{\sigma} = -a_9a_{10}x_6 - b_4u_b - a_7\dot{x}_5 + f_\sigma(N_M, \phi) \tag{24}$$

where $f_\sigma = \frac{\partial \dot{\sigma}}{\partial x_5}\dot{x}_5 + \frac{\partial \dot{\sigma}}{\partial x_7}\dot{x}_7 + \frac{\partial \dot{\sigma}}{\partial x_3}\dot{x}_3 + \frac{\partial \dot{\sigma}}{\partial x_4}\dot{x}_4$ contains all the uncertainties of Δ_1 and others known terms, is evident that second derivative is very hard to be computed due to that is highly nonlinear. Therefore, it is not easy to use common techniques to design a robust controller. In order to achieve chattering reduced sliding mode motion on the manifold $\sigma = \dot{\sigma} = 0$, we use the high order sliding mode technique presented in [2]. Thus, the control input is proposed in the form:

$$u_b = \frac{\alpha}{b_3}\left(0.5 + 0.5\text{sign}(\dot{\sigma} + \beta\,|\sigma|^{1/2}\,\text{sign}\sigma)\right) \qquad (25)$$

with $\alpha, \beta > 0$. The control signal (25) establishes a 2-sliding mode $\sigma = \dot{\sigma} = 0$ attracting each trajectory in finite time [18].

In order to use the controller (25) we need to know the time derivative $\dot{\sigma}$ of the output tracking error. Note that to compute that derivative of σ is not an easy task, to avoid this calculation and considering σ is known, we propose to use a the first-order differentiator [19], [20] for the estimation of $\dot{\sigma}$. In this case, the differentiator is in the form

$$\begin{aligned} \dot{z}_0 &= -\lambda_1 L^{1/2}\,|\epsilon|^{1/2}\,\text{sign}\,(\epsilon) + z_1 \\ \dot{z}_1 &= -\lambda_0 L\text{sign}\,(\epsilon) \end{aligned} \qquad (26)$$

where $\epsilon = \sigma - z_0$ and z_0 and z_1 are estimations of σ and $\dot{\sigma}$ respectively.

IV. SIMULATION RESULTS

To show the performance of the proposed control laws (17), (25), we have carried out simulations on a wheel and active suspension model, the system parameters used for the simulations are listed in Table 1.

During the breaking process we want to maximize the friction force, for that reason throughout simulations we suppose that slip tracks a constant signal $s^* = 0.203$, which in this case produces a value close to the maximum of the function $\phi(s)$. The reference for suspension is $y_{1d} = -0.2$. The road perturbation is considered as $z_r = 0.1\cos(10t)$. The parameters used in the control law are $\lambda_{s1} = 10$, $\lambda_{s2} = 15$, $\mathbf{C}_1 = \begin{bmatrix} -175 & -35 & 0 \end{bmatrix}^T$, $\alpha = 10000$, $\beta = 5000$, $\lambda_0 = 1.1$, $\lambda_1 = 1.5$, $L = 1000$.

On the other hand, to show robustness properties of the control algorithms in presence of parametric variations we introduce a change of the friction coefficient ν which produces different contact forces, that is F and $\hat{F}$. Then, $\nu = 0.1$ for $t < 4$ s and $\nu = 0.5$ for $t \geq 4$ s.

Longitudinal speed v and the linear wheel speed $r\omega$ are shown in Fig. 3, the ABS controller should be turned off when the longitudinal speed is close to zero.

TABLE 1
Values of Parameters (MKS Units)

Parameter	Value	Parameter	Value	Parameter	Value
m_c	1800	J	18.9	E	0.97
m_w	50	k_b	100	A_f	6.6
K_{cw}	1050	b_b	0.08	C_d	0.65
K_{wr}	175500	r	0.535	ρ	1.225
C_{cw}	19960	B	10	v_w	-6
C_{wr}	1500	C	1.9	g	9.81
τ	0.0043	D	1	v	0.5

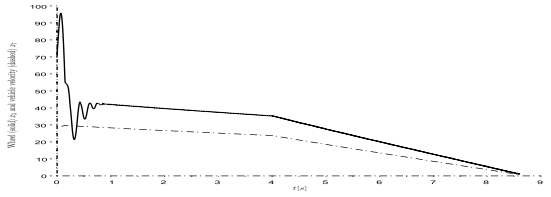

Fig. 3: Longitudinal speed v (dashed) and the linear wheel speed $r\omega$ (solid)

The Fig. 4 shows the slip rate during the breaking process, we can see the fast convergence to the reference value s^* and Fig. 5 presents the friction/slip characteristic relation $\phi(s)$ obtained during the breaking process under control actions.

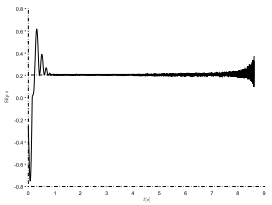

Fig. 4: Slip performance in the braking process

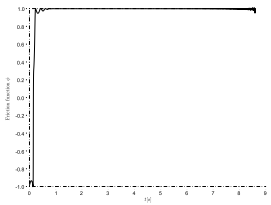

Fig. 5: Performance of $\phi(s)$ in the braking process

Fig. 6 shows the vertical vehicle position during the breaking process.

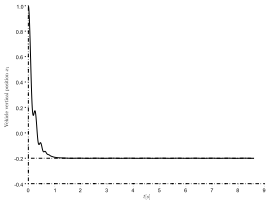

Fig. 6: Vehicle position x_1

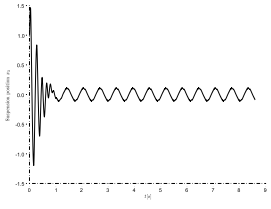

Fig. 7: Suspension position x_3

We could see the position is lowered 0.2 m under zero position and that is kept constant until the car is almost

stopped, until Fig. 7 presents the suspension position of the vehicle, we note that moves constantly trying to counteract the changes on the road and wheel.

The control action u_s for the suspension is shown in Fig. 8. Note that the valve can put or extract fluid into the reservoir to obtain the necessary forces. The sliding variable ψ is presented in figure 9.

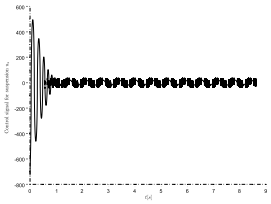

Fig. 8: Control signal for suspension u_s

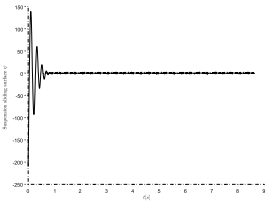

Fig. 9: Sliding surface for suspension control ψ

The control signal u_b for the ABS system is presented in Fig. 8, due to the form of the control design (25) the control signal is switching between two values. The sliding variable σ is presented in figure 11.

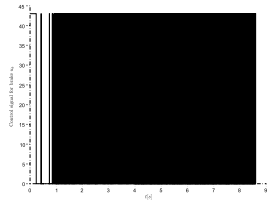

Fig. 10: Control signal for ABS u_b

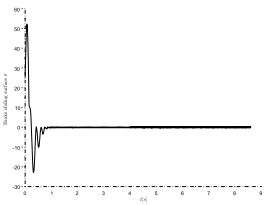

Fig. 11: Sliding surface for ABS control σ

Finally, in Fig. 12 the nominal F, and the $\hat{F}$ contact forces are shown

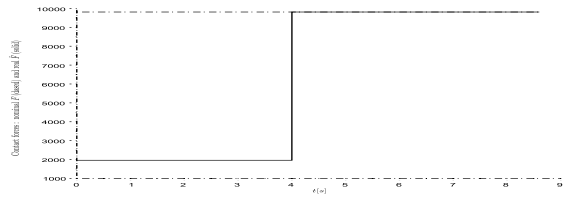

Fig. 12: Nominal contact force F (dashed) and real force $\hat{F}$ (solid)

V. CONCLUSIONS

In this work high order sliding mode based controller for ABS assisted with active suspension has been proposed. To overcome the difficulty of the calculation of the derivatives needed for the HOSM ABS control, SM differentiator were used. The simulation results show good performance and robustness of the closed-loop system in presence of both, the matched and unmatched perturbations, namely, parametric variations and neglected dynamics.

References

[1] V. Utkin, J. Guldner, and J. Shi, *Sliding Mode Control in Electro-Mechanical Systems, Second Edition (Automation and Control Engineering)*, 2nd ed. CRC Press, 5 2009.

[2] A. Levant, "Higher-order sliding modes, differentiation and output-feedback control," *Int. J. of Control*, vol. 76, no. 9/10, pp. 924–941, 2003, special issue on Sliding-Mode Control.

[3] H. Tan and Y. Chin, "Vehicle traction control: variable structure control approach," *Journal of Dynamic Systems, measurement and Control*, vol. 113, pp. 223–230, 1991.

[4] S. Drakunov, U. Ozguner, P. Dix, and B. Ashrafi, "ABS control using optimum search via sliding modes," *IEEE Transactions on Control Systems Technology*, vol. 3, no. 1, pp. 79–85, 1995.

[5] C. Unsal and P. Kachroo, "Sliding mode measurement feedback control for antilock braking systems," *IEEE Transactions on Control Systems Technology*, vol. 7, no. 2, pp. 271–278, 1999.

[6] W. Ming-Chin and S. Ming-Chang, "Simulated and experimental study of hydraulic anti-lock braking system using sliding-mode PWM control," *Mechatronics*, vol. 13, pp. 331–351, 2003.

[7] Y. M. Sam, J. H. S. Osman, and M. R. A. Ghani, "A class of proportional-integral sliding mode control with application to active suspension system," *Systems & Control Letters*, vol. 51, no. 3-4, pp. 217 – 223, 2004.

[8] J. Lin and W. Ting, "Nonlinear control design of anti-lock braking systems with assistance of active suspension," *IET Control Theory & Applications*, vol. 1, no. 1, pp. 343–348, 2007.

[9] A. G. Loukyanov and V. I. Utkin, "Methods of reducing equations for dynamic systems to a regular form," *Automation and Remote Control*, vol. 42, no. 4, pp. 413–420, 1981.

[10] W. M. Wonham, *Linear Multivariable Control: A Geometric Approach*, 2nd ed. Springer, 1979.

[11] C. Clover and J. Bernard, "Longitudinal tire dynamics," *Vehicle System Dynamics*, vol. 29, pp. 231–259, 1998.

[12] S. Jansen, P. Zegelaar, and H. Pacejka, "The influence of in-plane tyre dynamics on ABS braking of a quarter vehicle model," *Vehicle System Dynamics*, vol. 32, no. 2, pp. 249–261, 1998.

[13] I. Novozhilov, P. Kruchinin, and M. Magomedov, "Contact force relation between the wheel and the contact surface," *Collection of scientific and methodic papers Teoreticheskaya mekhanika, MSU*, vol. 23, pp. 86–95, 2000, (In Russian).

[14] P. Kruchinin, M. Magomedov, and I. Novozhilov, "Mathematical model of an automobile wheel for antilock modes of motion." *Mechanics of Solids*, vol. 36, no. 6, pp. 52–57, 2001.

[15] E. Bakker, H. Pacejka, and L. Lidner, "A new tire model with application in vehicle dynamic studies," *SAE Paper No. 890087*, vol. 01, pp. 101–113, 1989.

[16] W. Perruquetti and J.-P. Barbot, *Sliding Mode Control In Engineering (Automation and Control Engineering)*, 1st ed. CRC Press, 1 2002.

[17] A. Polyakov and A. Poznyak, "Reaching time estimation for "super-twisting" second order sliding mode controller via Lyapunov function designing," *IEEE Transactions on Automatic Control*, vol. 54, no. 8, pp. 1951–1955, 2009.

[18] A. Levant, "Homogeneity approach to high-order sliding mode design," *Automatica*, vol. 41, no. 5, pp. 823 – 830, 2005.

[19] ——, "Robust exact differentiation via sliding mode technique," *Automatica*, vol. 34, no. 3, pp. 379 – 384, 1998.

[20] M. T. Angulo, L. Fridman, and A. Levant, "Robust exact finite-time output based control using high-order sliding modes," *Intern. J. Syst. Sci.*, vol. 0, p. 0, 2011.